Preliminary Results from Ensemble Data assimilation of the Martian Atmosphere using TES radiances

C. Lee[1], M. I. Richardson[1], W. G. Lawson[2], J. L. Anderson[3], N. Collins[3],
T. Hoar[3], M. Mischna[4], A. D. Toigo[5]
1:Ashima Research, 2: Point Carbon, 3: UCAR, 4: JPL, 5: Cornell

ASHIMA RESEARCH
lee@ashimaresearch.com

Introduction

We have developed a new ensemble data assimilation scheme using the Data Assimilation Research Testbed (DART; Anderson, 2009) and the Mars version of the Weather Research and Forecast model (MarsWRF; Richardson et al., 2007). The combined system operates an Ensemble Kalman filter using MarsWRF to integrate the atmospheric state and DART to perform the analysis and innovation steps. A custom radiance forward model is used to ingest calibrated radiance data from the Thermal Emission Spectrometer (TES; Christensen et al., 2001) and modify a state vector that includes air and surface temperature, surface radiative and thermal properties, column dust optical depth, and horizontal winds.

In ingesting calibrated radiance data instead of retrieved temperature we remove a significant source of ambiguity from the assimilation (that of the retrieval model parameters, and its accuracy and precision) and obtain more information on the atmospheric state than is available in the temperature field alone. The radiances observed by TES provide information on the atmospheric thermal structure, the column dust opacity, the surface temperature and ice coverage (through albedo and emissivity), the ice-free surface thermal properties, atmospheric water ice, and co_2 ice clouds.

The MarsWRF GCM provides a well calibrated climatological Martian atmosphere, validated using the Viking lander pressure data (Guo et al., 2008) and diurnal thermal tides derived from temperature data retrieved from the Mars Climate Sounder (McCleese et al., 2009) and TES observations (Lee et al., 2009). We use a version of MarsWRF that is unmodified from the 'nominal' equivalent that reproduces the gross state of the Martian atmosphere (Richardson et al., 2007).

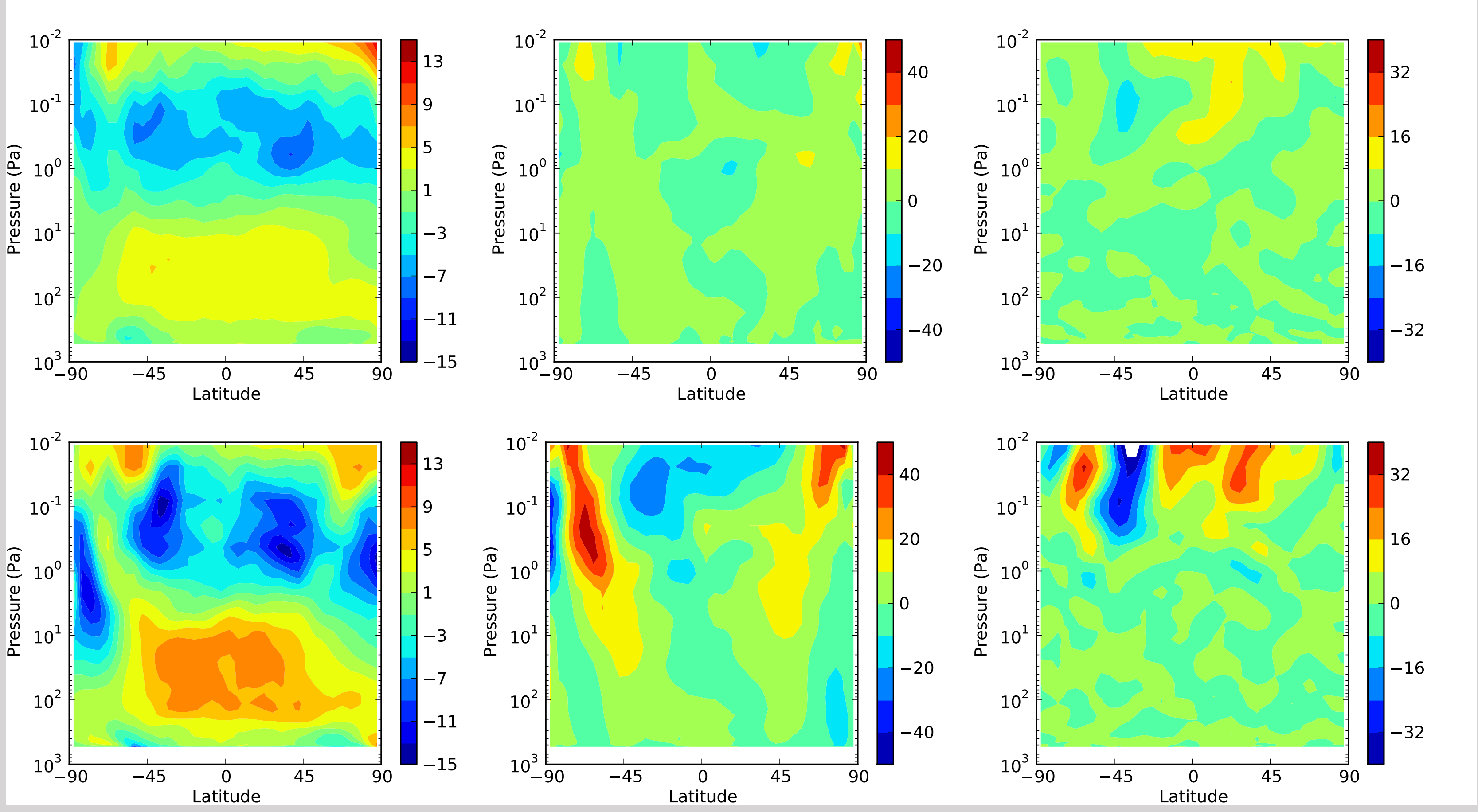

Figure 1: Affect of the assimilation on the atmospheric circulation.
Longitudinal mean differences between the assimilated GCM and the nominal GCM in the temperature field (left, K), the eastward wind (middle, m/s), and the northward wind (right, m/s) at the start (top) and end (bottom) of the assimilation.

The assimilation warms the lower atmosphere while cooling the upper atmosphere, resulting in a less stable atmosphere. The broad structure of the changes made by the assimilation suggests that the dust vertical distribution should be modified to alter the thermal stability of the atmosphere. Atmospheric dust is the dominant mechanism available in the model to control the vertical thermal structure.

At the same time, the horizontal thermal gradients are altered, the eastward mid-latitude jets are strengthened, and the south polar jet is moved southward . The changes to the northward winds are small in the bulk atmosphere in comparison to the eastward winds, but there is significant additional convergence at the top of the southern polar jet, and a strengthening of the meridional overturning near the top of the domain.

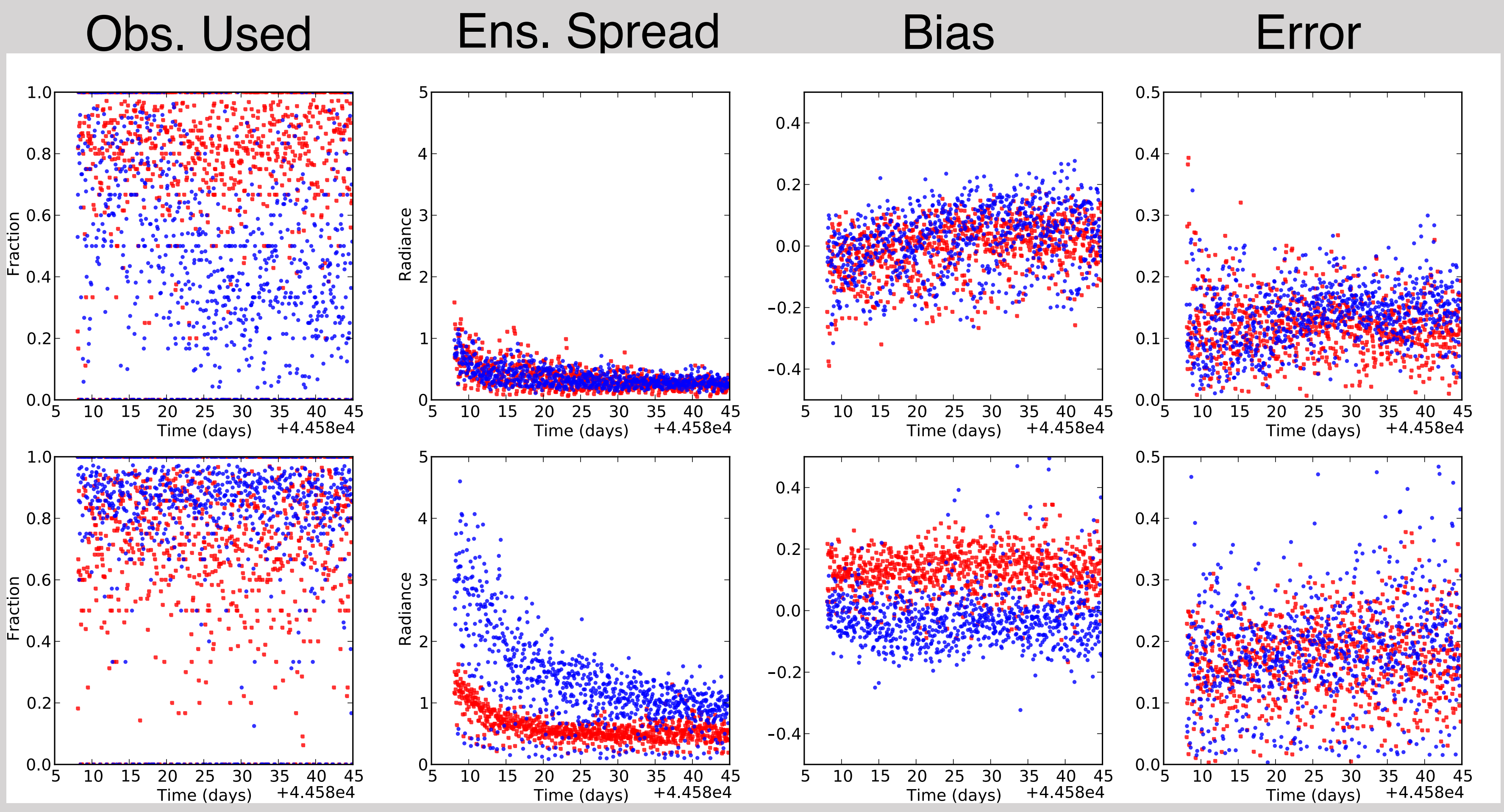

Figure 3: Ensemble performance during the assimilation
Progress of the assimilation plotted at each hourly assimilation step for two bands (top: atmosphere, bottom: surface), showing the (left-to-right) fraction of possible observation used, ensemble spread in radiance (10^{-2} $mW/m^2/str/cm^{-1}$), ensemble-observation bias ($mW/m^2/str/cm^{-1}$), and RMS error ($mW/m^2/str/cm^{-1}$). Day-time (blue) and night-time(red) data are shown.

The assimilation adjusts the model state to reduce the bias between the ensemble and observations, and is particularly successful in the free atmosphere (top panel). In the surface band (bottom panel) the day-night difference is dominated by an unmodified surface parameter, possibly soil thermal inertia or thermal conductivity, resulting in an underestimate of the diurnal cycle amplitude (over-estimating the night-time low temperature, under-estimating the day-time high temperature).

The ensemble loses some skill in the day-time atmosphere during the assimilation, caused by a lack of intrinsic variability (Newman et al., 2001) and lack of intra-ensemble dust variability. As the ensemble loses skill, the bias (relative to the ensemble spread) increases and causes DART to reject more observations based on the ensemble prediction, resulting in the model returning to its climatological state rather than the observationally constrained `weather’ driven state.

Some of the loss of skill will be mitigated using a new version of MarsWRF that includes improved parameterizations of the atmospheric physics, including advected dust, water ice clouds, and gravity wave drag.

References

Anderson, J. L. et al. (2009) ,BAMS, 1283-1296
Guo, X. et al. (2010), JGR Planets, 114:7, E07006
Lee et al., (2009), JGR Planets, 114: E03005
Newman et al., (2004), QJRMS, 10.1256/qj.03.209
McCleese et al., (2007), JGR Planets, 112:E5, E05S06
Richardson et al. (2007),JGR Planets, 112, E09001
Christensen, P. R. et al. (2001) JGR Planets 106 (E10): 23823-23872

Assimilation Details

The assimilation presented here uses 1.3 million TES radiance observations taken between July and August 1999 (Mars Ls 150-160), corresponding to late northern summer. We use 24 different radiance bands from each observation and collate all of the observations to a spatial resolution comparable with the GCM.

MarsWRF is integrated to the start of the assimilation and perturbed to provide an initial 20 member ensemble. The assimilation step is performed hourly using the appropriate TES observations to update the GCM atmosphere by combining observations and simulation using a Bayesian algorithm to optimally ingest the available information.

During the assimilation we calculate and retain the prior and posterior predictions of the observed state, and use this information to gauge the accuracy and precision of the assimilation. We also retain the complete atmospheric state produced by each ensemble member which allows us to characterize the intrinsic variability within the atmosphere and identify the causes of differences between the assimilated model state and the nominal un-assimilated model state.

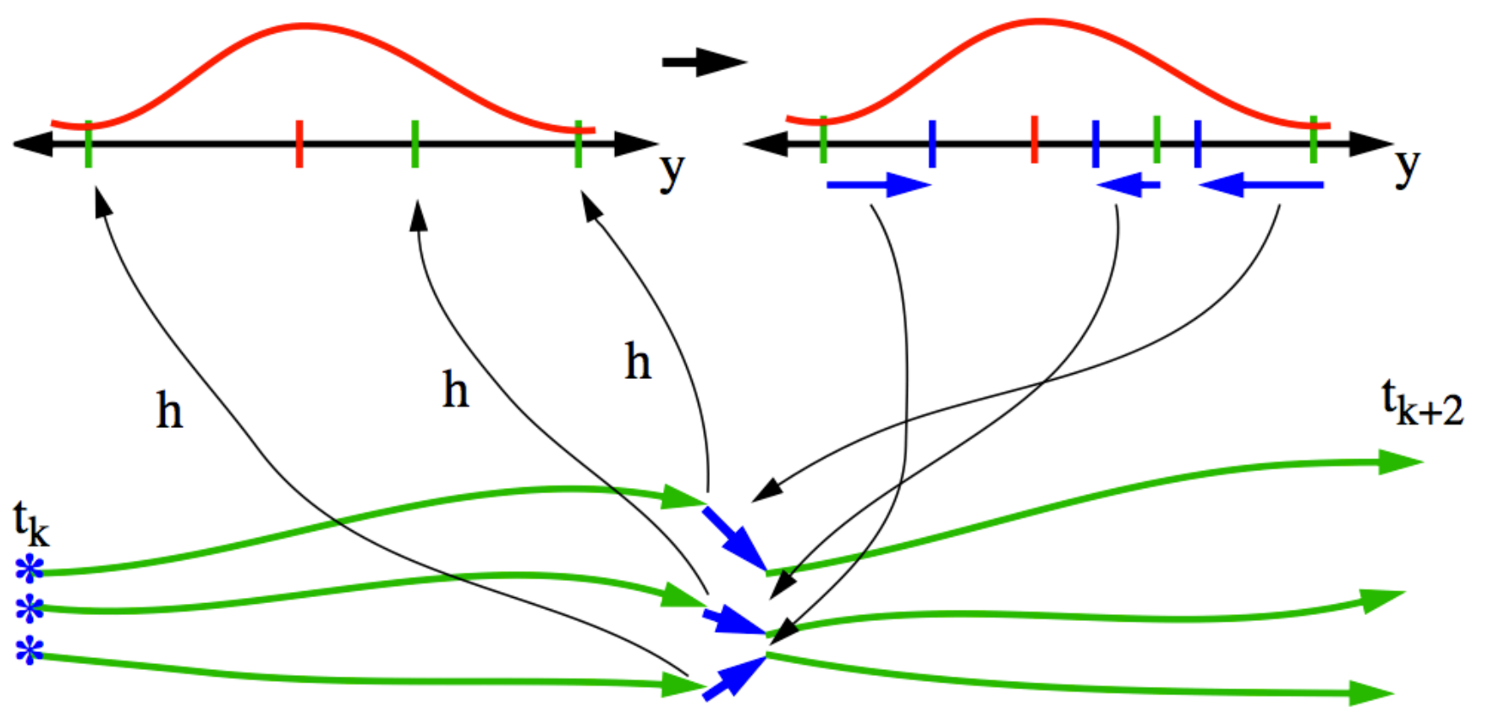

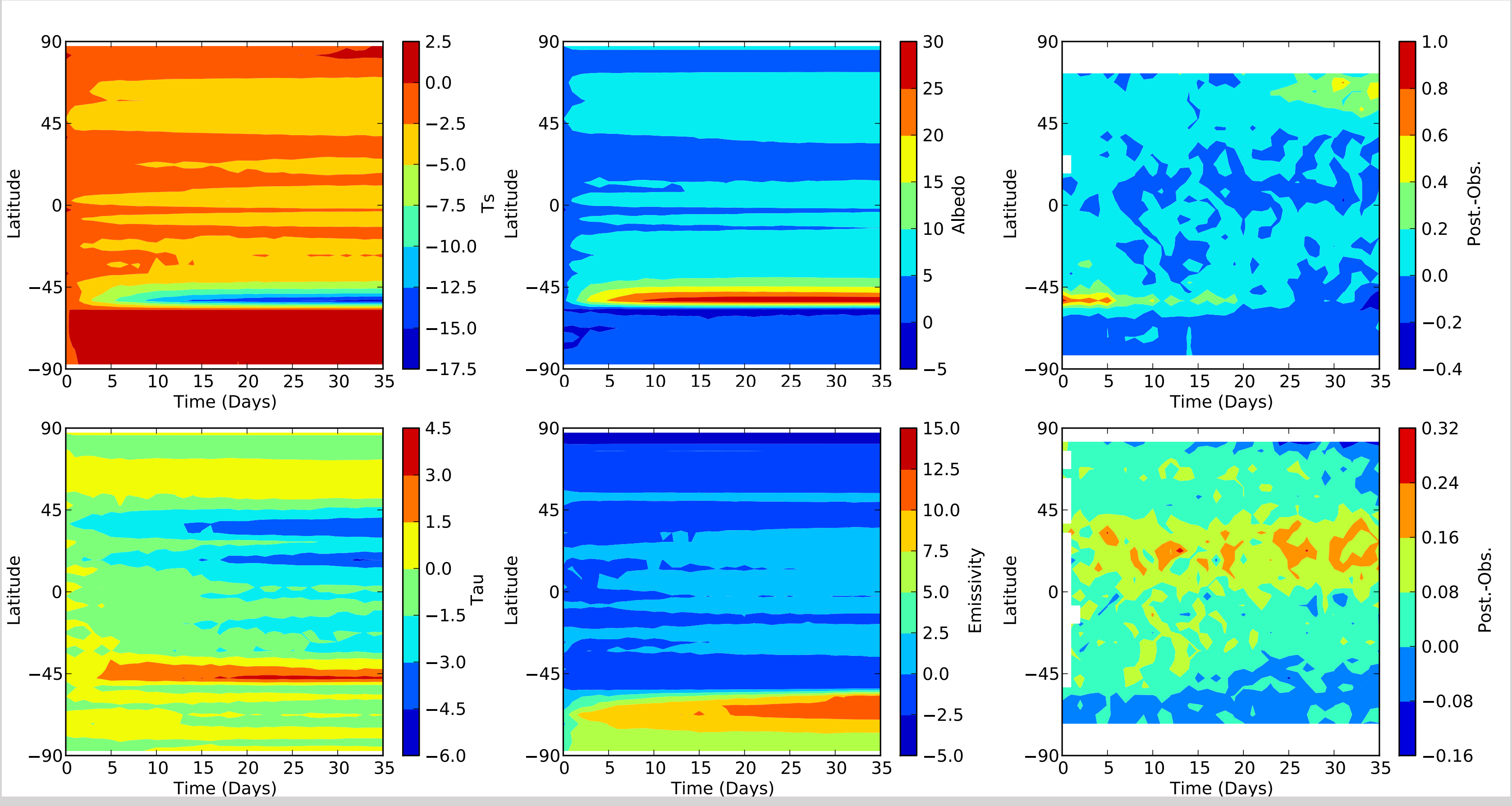

Figure 2: Affect of the assimilation on surface and dust parameters
Longitudinally averaged differences between the ensemble mean state from the assimilation and a 'nominal' model run without assimilation input. (top row) Change in surface temperature (K), surface visible albedo (%), PM Posterior-Observation surface bias in the assimilation ($mW/m^2/str/cm^{-1}$). (bottom row) change in column dust optical depth (0.01 opacity units), change in surface infra-red emissivity (%), AM Posterior-Observation surface bias in the assimilation ($mW/m^2/str/cm^{-1}$).

Within 5 days of the start of the assimilation, the bright radiance bias at the ice edge is corrected by increasing the dust opacity and increasing the surface albedo by 30% (almost the same as the ice-free to ice-covered difference). As a result, the ensemble bias disappears and very little large scale correction occurs until the end of the assimilation when the Northern polar cap begins to form.

The emissivity of the ice covered south pole is altered by 15% by the assimilation, possibly reflecting the sublimation of the ice during this time, or a correction to the prescribed ice emissivity in the model. The dust optical depth is reduced over Tharsis and Olympus Mons and increased over the southern edge of the newly forming north polar cap.

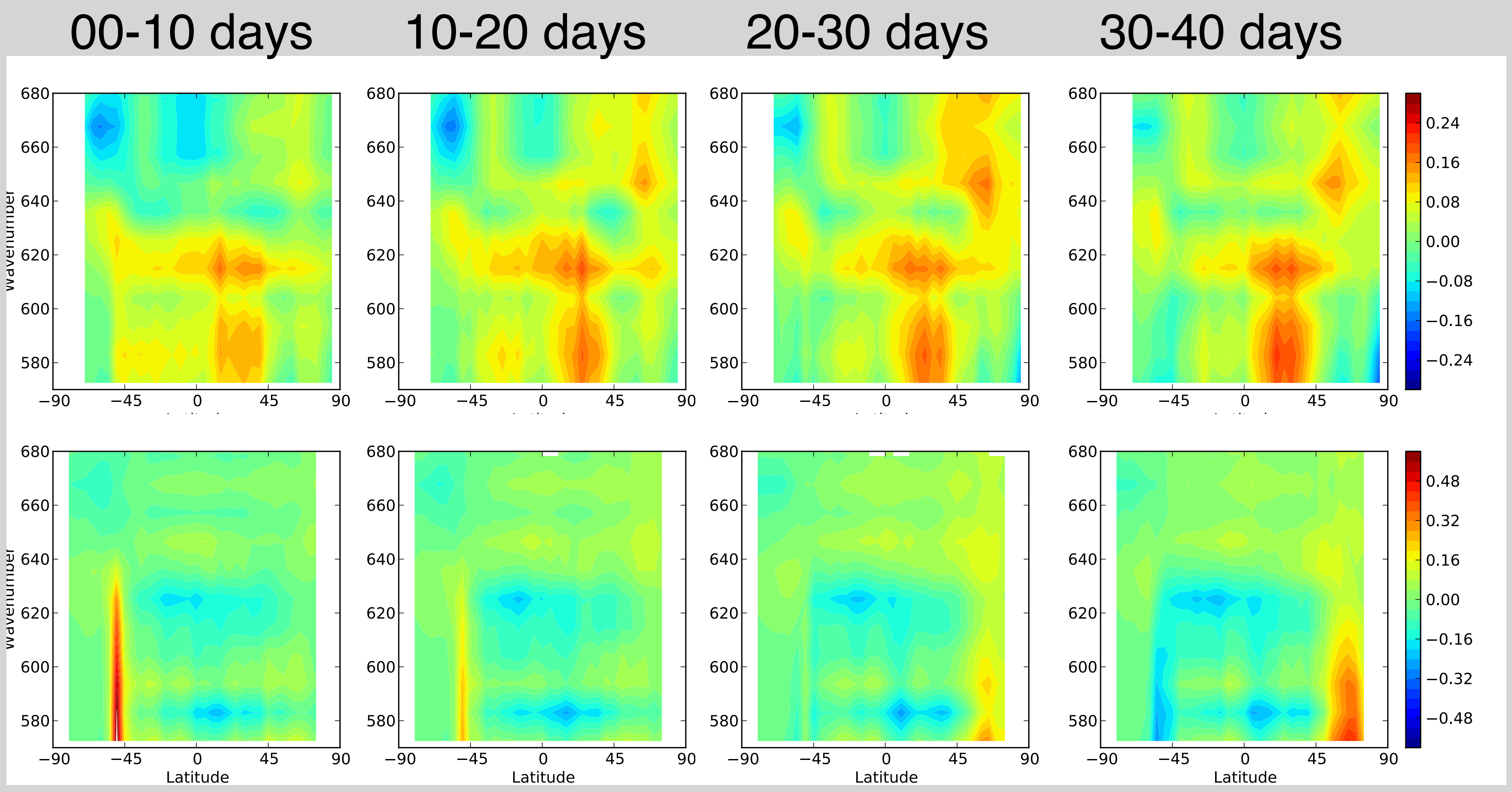

Figure 4: Ensemble biases corrected by the assimilation
Mean biases (ensemble mean - observations) for the 40 days of assimilation, plotted as a function of latitude and observation wavenumber (a proxy of altitude), shown for the night-time (top) and day-time (bottom) atmosphere.

The radiance from ice edge at 45 south is initially over-predicted, but is quickly corrected by the assimilation as the ice edge is modified and dust is injected into the atmosphere as shown in figure 2. The remaining bias, in the ice-free atmosphere (north of 45 South) is dominated by the diurnal bias shown in figure 3, but has an additional weak dependence on the topography (Olympus Mons at 30 North, Hellas basin at 30 South). The structure of these biases suggest changes are required to the surface thermal properties and dust columns over extreme topography.

Conclusions

The ensemble data assimilation scheme we have developed is able to efficiently ingest calibrated radiance data from TES using a radiance forward model to simulate observations from the MarsWRF predicted atmosphere. The assimilation scheme quickly corrects discrepancies between the climatological state and the true atmospheric state modified by short term weather systems and variability in the Martian atmosphere. The assimilation scheme also helps us to identify errors in the prescribed fields (such as surface thermal properties) and the physical parameterizations (the predicted dust lifting locations and vertical profiles) used in the GCM and gives a quantitative measure of their prospective solutions.

The GCM, forward model, and data assimilation interface used in this project are being prepared for public release to allow researchers to use the powerful tools available in DART to improve our knowledge of the Martian system. A tutorial based on the data presented here will be made available to guide the user in the data assimilation process.